Bioorganic & Medicinal Chemistry Letters 18 (2008) 6210–6213

Contents lists available at ScienceDirect

Bioorganic & Medicinal Chemistry Letters

journal homepage: www.elsevier.com/locate/bmcl

Naphthalimide intercalators with chiral amino side chains: Effects of chirality on DNA binding, photodamage and antitumor cytotoxicity

Qing Yang [a,*], Peng Yang [a], Xuhong Qian [c,*], Lianpeng Tong [b]

[a] Department of Bioscience and Biotechnology, Dalian University of Technology, No. 2 Linggong Road, Ganjingzi, Dalian, Liaoning Province 116012, China
[b] State Key Laboratory of Fine Chemicals, Dalian University of Technology, Dalian 116012, China
[c] Shanghai Key Laboratory of Chemical Biology, East China University of Science and Technology, Shanghai 200237, China

ARTICLE INFO

Article history:
Received 13 July 2008
Revised 19 September 2008
Accepted 30 September 2008
Available online 5 October 2008

Keywords:
Antitumor agents
Chirality
Naphthalimide
DNA intercalation
DNA photodamage

ABSTRACT

Several novel heterocyclic-fused naphthalimides intercalators with chiral amino side chains were investigated. Their side chains' chiral configuration determines DNA binding activities in the order: *S*-enantiomers > *R*-enantiomers. And their DNA photodamaging activities were in good agreement with their DNA binding constants, the *S*-enantiomers could photocleave circular supercoiled pBR322 DNA more efficiently than their *R*-enantiomers. *S*-enantiomer $\mathbf{B}^3$ could photodamage DNA at 0.2 μM and cleave supercoiled plasmid DNA from form I to form II completely at 50 μM. Almost all of these intercalators showed effective cytoxicities against human lung cancer cells and murine leukemia cells. *S*-enantiomers showed different antitumor cytotoxicity by comparison with *R*-enantiomers. This work may provide additional information for the role of amino side chains on intercalators as antitumor agents.

DNA intercalating agents as major class of antitumor compounds have received most and continued attention. They usually function as DNA-targeted topoisomerase I and/or II inhibitors. Usually these agents are characterized by the presence of a tri- or tetracylic annelated planar and aromatic ring capable of inserting the nucleic acid bases[5] and one or two flexible amino side chains for promoting DNA affinity through electrostatic or hydrophobic interactions.[1–3] *N*,*N*-dimethyl alkyldiamino group and its analogues, for example, are widely applied as anticancer agents in conjugation with an intercalating moiety including anthraquinone, acridine, benzimidazole-quinoline, fluorenone, pyridine-diones, naphthalimides, etc.[2,4] (Fig. 1).

Up to now, little is known for interactions between chiral intercalators and DNAs,[5,6] let alone effects of chirality of amino side chains on DNA binding ability, photodamage activity as well as antitumor cytotoxicity. However, chirality plays very important roles in biological system. DNA itself is a chiral molecule with right-handed helical configuration. The helical grooves of DNA were considered to be the most pronounced enantio-selectivity part, while the insertion of chiral moiety between the achiral DNA bases is generally believed to contribute less enantioselectivity.[5,7–10]

Naphthalimides are well-known DNA photocleavers[11], and naphthalimides bearing side chains are well-known antitumor agents against a variety of murine and human tumor cells.[7] However, less investigation on naphthalimides with chiral amino side chains has been performed. We ever reported heterocyclic naphthalimides with achiral amino side chains as highly efficient artificial nucleases and antitumor agents.[12] In this study, we report a series of bioactive heterocylclic naphthalimides with chiral amino side chains (Fig. 2). Here, racemic (X), chiral (*R*)-(+)- and (*S*)-(−)-*N*-ethyl–2-(aminomethyl) pyrrolidine (*R*, *S*, respectively) are side chains.

The synthesis of $\mathbf{A}^n$, $\mathbf{B}^n$, $\mathbf{C}^n$ and $\mathbf{D}^n$ (n = X, *R*, *S*) was carried out by the condensation reaction of the corresponding anhydride ($\mathbf{A}^0$, $\mathbf{B}^0$, $\mathbf{C}^0$ and $\mathbf{D}^0$) with amine, starting from 4-bromo-3-nitro or 4-bromo-1,8-naphthalic anhydride. The synthesis strategies were outlined in Figure 3.[13–15] Their structures were confirmed by IR, ^{1}H NMR and HRMS.[16]

The Scatchard binding constants for calf thymus DNA (CT-DNA) were monitored by fluorescence spectroscopy (in 30 mM Tris–HCl buffer, pH 7.0).[17] Table 1 listed their detailed UV–Vis, fluorescence data, Scatchard binding constants and anticancer activities. It indicated the Scatchard binding constants of *S*-enantiomers were higher than those of the corresponding *R*-enantiomers as well as those of the racemic ones. The order of their Scatchard binding constants was: (1) **B** > **C** > **D** > **A** for compounds, which was related to the introduction of a sulphur atom into these molecules, and (2) *S* > X > *R* for configuration.

DNA binding affinity is known to be determined by several actions including groove binding, DNA intercalation and electrostatic

* Corresponding authors. Tel./fax: +86 411 84709687 (Q.Y.).
E-mail addresses: qingyang@dlut.edu.cn (Q. Yang), xhqian@ecust.edu.cn (X. Qian).

0960-894X/$ - see front matter © 2008 Elsevier Ltd. All rights reserved.
doi:10.1016/j.bmcl.2008.09.104

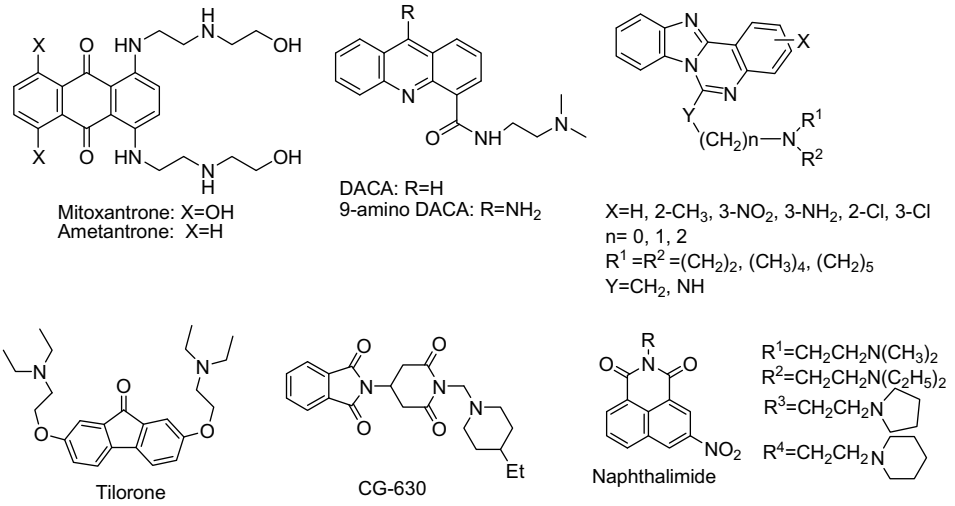

Figure 1. Intercalating moieties and amino side chains of well-known antitumor agents.

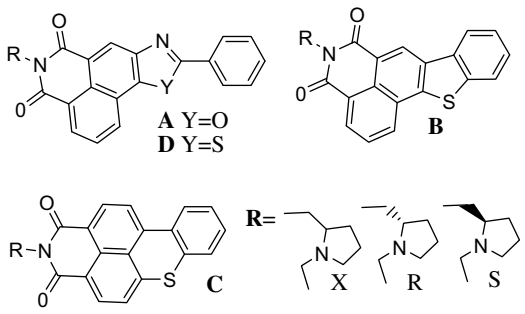

Figure 2. Heterocyclic-fused naphthalimide chiral amino side chains.

binding. For those which carry the same intercalative moiety, their DNA binding affinity differences mainly come from electrostatic interactions between amino side chains and DNAs. Preferential and average binding value of these enantiomers was K(*R*)/K(*S*) ≈ 0.5, which is in very similar with Becker's investigation for both the anthracene and the pyrene compounds[5], although the Becker's structure is quite different from these molecules. The slight enantiomeric preference was explained in terms of orientation polarity during the binding, by which any intrinsic enantioselectivity is canceled by averaging of opposite binding orientations.[5]

DNA photocleavage activities of these chiral DNA intercalators were evaluated. In the dark, they did not promote DNA strand breaking. Being irradiated under 365 nm light, the DNA cleavage ability of *S*-enantiomers was by far higher than that of *R*-enantiomers. The order of DNA cleavage efficiency by these compounds was determined to be *S* > X > *R* and $\mathbf{B^n} > \mathbf{C^n} > \mathbf{D^n} > \mathbf{A^n}$, which were almost parallel with their DNA binding abilities. To the best of our knowledge, this is the first report for the difference between *S*- and *R*-enantiomers of photo-activated naphthalimides. It could be concluded the *S*-amino side chain showed greater potential in developing novel DNA intercalators with higher DNA binding and in turn DNA cleavage efficiency.

Figure 4 showed the concentration dependence of DNA photocleavage efficiencies. $\mathbf{A^S}$ at 0.5 μM could damage supercoiled plasmid DNA pBR322 (Fig. 4c), while under 1 h light exposure, 0.2 μM of $\mathbf{B^S}$ and 0.5 μM of $\mathbf{C^S}$ started to cleave DNA (Fig. 4d, 4f). The *R*-enantiomer $\mathbf{B^R}$ could cleave DNA at 5 μM but could not converse Form I completely to Form II even when its concentration reached 50 μM (Fig. 4e), however, *S*-enantiomer $\mathbf{B^S}$ could cleave plasmid DNA from

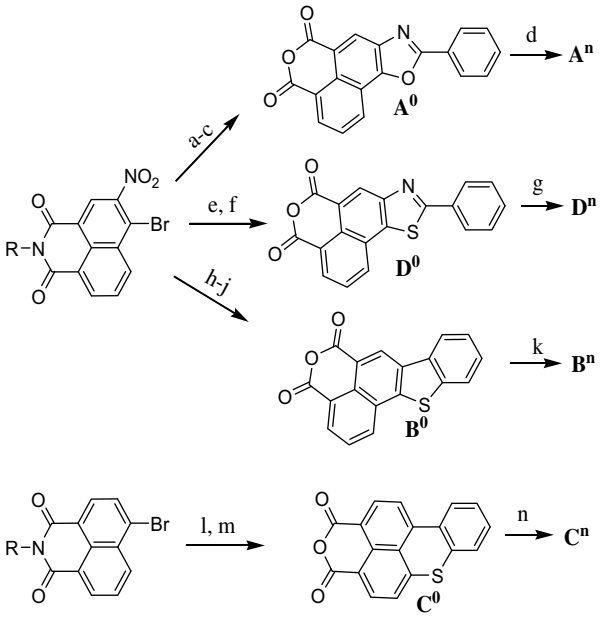

Figure 3. Synthesis routes summary. (a) NaOH, H_2O, 80–85 °C, 8 h, 85% yield; (b) $SnCl_2$, HCl, 80 °C, 6 h, 66% yield; (c) PPA, benzoic acid, 135 °C, 4 h, 62% yield; (d) RNH_2, ethanol, reflux, 3 h, 85% yield; (e) NaS_2, S, 100 °C, 8 h; (f) benzaldehyde, acetic acid, N_2, 6 h, 60% yield; (g) RNH_2, ethanol, reflux, 3 h, 85% yield; (h) PhSH, EtOH, reflux, 4 h, 97% yield; (i) $SnCl_2$/concentrated HCl, 96% yield; (j) Pochorr cyclisation: $NaNO_2$, H_2O–HCl–HOAc, 0–5 °C, 2 h; $CuSO_4$, HOAc, reflux, 2 h, 64% yield; (k) RNH_2, ethanol, reflux, 3 h, 83% yield; (l) 2-aminobenzenethiol, K_2CO_3, DMF, reflux, 30 min, 77% yield; (m) Pochorr cyclisation: $NaNO_2$, HOAc, H_2SO_4; $CuSO_4$, HOAc, H_2O, 99% yield; (n) RNH_2, ethanol, reflux, 3 h, 85% yield.

form I to form II by 100% at 50 μM (Fig. 4d). The order of DNA cleavage efficiency by these chiral compounds was $\mathbf{B^S} > \mathbf{C^S} > \mathbf{A^S}$.

Mechanism experiments were performed by adding different scavengers (Fig. 5). Taking $\mathbf{A^S}$, $\mathbf{B^S}$, $\mathbf{C^S}$ as examples (Fig. 5a, b and d), histidine (singlet oxygen quencher) and ethanol (hydroxyl radical scavenger) had no obvious effect on photocleavage efficiency, indicating that singlet oxygen and hydroxyl radical were not likely to be involved in the cleaving species. However, the DNA-cleaving activity of $\mathbf{A^S}$, $\mathbf{B^S}$, $\mathbf{C^S}$ decreased dramatically in the presence of DTT (dithiothreitol, superoxide anion scavenger). DTT could retard the superoxide anion radicals, which might form after oxygen was activated by accepting an electron transferred from nucleobase to

Table 1
Spectra data, photocleaving activity, and cytotoxicity

	UV/nm (lgε)	FL/nm (Φ)	Ka ($\times 10^5$ M^{-1})	K_R/K	IC_{50} (μM)	
					A549	P388
$\mathbf{A^x}$	375 (3.10)	428 (0.0089)	1.24		2220	383
$\mathbf{A^R}$	375 (3.63)	430 (0.0144)	0.82		0.89	13.9
$\mathbf{A^S}$	375 (3.61)	429 (0.0184)	1.62	0.51	2.72	4.82
$\mathbf{B^x}$	381 (3.94)	454 (0.0205)	9.07		2.88	0.47
$\mathbf{B^R}$	381 (3.77)	454 (0.0231)	6.23		6.02	2.28
$\mathbf{B^S}$	381 (3.75)	454 (0.0216)	10.0	0.62	0.58	4.90
$\mathbf{C^x}$	469 (3.81)	522 (0.1805)	3.02		0.49	12.2
$\mathbf{C^R}$	469 (3.57)	522 (0.1501)	2.51		8.84	12.3
$\mathbf{C^S}$	469 (4.24)	523 (0.1311)	6.10	0.41	0.57	5.11
$\mathbf{D^x}$	315 (4.47)	429 (0.0056)	2.32		0.16	0.59
$\mathbf{D^R}$	315 (4.42)	429 (0.0022)	1.23		0.07	3.35
$\mathbf{D^S}$	315 (3.98)	429 (0.0072)	2.85	0.43	0.23	1.17

intercalator. However, the addition of SOD (superoxidedimutase) did not obviously inhibit the DNA cleavage as DTT did. It was also found that there was no difference in photocleavage mechanism between *R*/*S*-enantiomers $\mathbf{B^R}$ and $\mathbf{B^S}$ (Fig. 5b and c).

The antitumor activities against human lung cancer cell (A549) and murine leukemia cell (P388) of these novel compounds with racemic, chiral (*R*)-(+)- and (*S*)-(−)-*N*-ethyl-2-(aminomethyl) pyrrolidine side chains, were evaluated by means of Sulforhodamine B (SRB) assay or MTT tetrazolium dye assay (in dark or under daily scattered light), respectively (Table 1). The racemic, (*R*)-(+)- or (*S*)-(−)-enantiomers showed different bioactivities, respectively. $\mathbf{B^x}$ and $\mathbf{D^x}$ showed the strong cytotoxicity for P388 (IC_{50}, 0.47 and 0.59 μM, respectively), $\mathbf{D^R}$ showed the highest cytotoxicity against A549 (IC_{50}, 0.07 μM). It could be found that the cyctotoxicities of racemic ones maybe lower or maybe higher than those of the corresponding *R*- or *S*-enantiomer alone. It implied that for *R*- and *S*-enantiomer, beside their different and competing actions with DNA and Topo II targets, there might be some unknown (positive or negative) mechanisms in cells, which strengthen or weaken the cytotoxicity of racemics.

Although there were no obvious or direct relationship between their cytotoxicities and DNA binding affinities, it was interesting that the chiral amino side chains did play a very important role in their antitumor cytotoxicities. *R*/*S*-enantiomers behaved quite differently in terms of cytotoxicity against different cell lines, suggesting that the chiralities of amino side chains is of special importance in developing novel antitumor agents.

In conclusion, the chirality of amino side chains of naphthalimides affect DNA binding affinity, DNA photocleavage activity as well as cytotoxicity, which might provide considerations for developing highly efficient DNA intercalators and better anti-tumor agents.

Acknowlegments

Financial support by the National Key Project for Basic Research (2003CB114400) and under the auspices of the National Natural Science Foundation of China (20536010) (20576016) (20676021) is greatly appreciated. The authors also thank for the support from

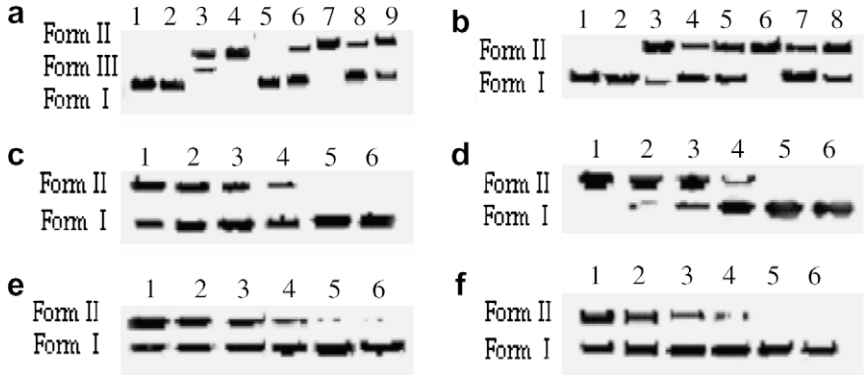

Figure 4. Photocleavage of supercoiled pBR322 DNA in the buffer of HEPES (20 mM, pH 7.0) containing 20% of acetonitrile under 365 nm light irradiation (a) DNA photocleavage by compounds (100 μM) for 1 h. Lane 1, DNA alone (hν), lane 2, DNA alone (no hν); lane 3–9, $\mathbf{A^0}$, $\mathbf{A^S}$, $\mathbf{A^R}$, $\mathbf{A^x}$, $\mathbf{D^S}$, $\mathbf{D^R}$, $\mathbf{D^x}$ and DNA, respectively; (b) DNA photocleavage by compounds (50 μM) for 1 h. (Lane 1) DNA alone (hν), (lane 2) DNA alone (no hν); (lane 3–8) $\mathbf{C^S}$, $\mathbf{C^R}$, $\mathbf{C^x}$, $\mathbf{B^S}$, $\mathbf{B^R}$, $\mathbf{B^x}$ and DNA, respectively; (c) DNA photocleavage by $\mathbf{A^s}$ at various concentrations for 2 h. (Lane 1–5) $\mathbf{A^s}$ at concentration of 50, 25, 10, 5, 0.5 μM, respectively, (lane 6) DNA alone (hν); (lane 7) DNA alone (no hν); (d) DNA photocleavage by $\mathbf{B^S}$ at various concentrations for 1 h. (Lane 1–5), $\mathbf{B^S}$ at concentration of 50, 25, 5, 0.2 μM, respectively, (lane 6), DNA alone (hν); lane 7, DNA alone (no hν); (e) DNA photocleavage by $\mathbf{B^R}$ at various concentrations for 1 h. (Lane 1–5), $\mathbf{B^R}$ at concentration of 50, 25, 10, 5 μM, respectively, Lane 6, DNA alone (hν); (lane 7), DNA alone (no hν); (f) DNA photocleavage by $\mathbf{C^S}$ at various concentrations for 1 h. Lane 1–5, $\mathbf{C^S}$ at concentration of 50, 25, 10, 0.5 μM, respectively, (lane 6), DNA alone (hν); (lane 7), DNA alone (no hν).

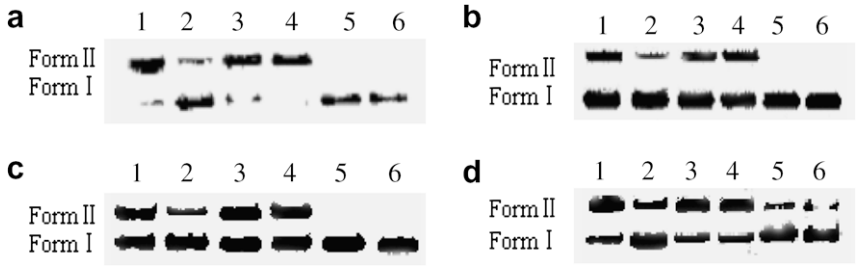

Figure 5. Mechanism experiments of photocleavage for $\mathbf{A^S}$, $\mathbf{B^S}$, $\mathbf{B^R}$ and $\mathbf{C^S}$. (a) (Lane 1–3) DNA and $\mathbf{A^S}$ in the presence of histidine (6 mM), dithiothreitol (DTT, 30 mM), ethanol (1.7 M), respectively; (lane 4), DNA and **As**; (lane 5) DNA alone (hν); (lane 6) DNA alone (no hν); (b) (lane 1–3), DNA and $\mathbf{B^S}$ in the presence of histidine (6 mM), DTT (30 mM), ethanol (1.7 M), respectively; (lane 4), DNA and $\mathbf{B^S}$; (lane 5), DNA alone (hν); (lane 6), DNA alone (no hν); (c) (lane 1–3), DNA and $\mathbf{B^R}$ in the presence of histidine (6 mM), DTT (30 mM), ethanol (1.7 M), respectively; (lane 4), DNA and $\mathbf{B^R}$; (lane 5), DNA alone (hν); (lane 6), DNA alone (no hν); (d) (lane 1–3), DNA and $\mathbf{C^S}$ in the presence of histidine (6 mM), DTT (30 mM), ethanol (1.7 M), respectively; (lane 4), DNA and $\mathbf{C^S}$; (lane 5), DNA alone (hν); (lane 6), DNA alone (no hν).

Fok Ying Tong Education Fund (101072), the State Key Laboratory of Bioreactor Engineering at East China University of Science and Technology, and Shanghai Institute of Organic Chemistry, Chinese Academy of Sciences, China.

References and notes

1. Behr, J. P. *Acc. Chem. Res.* **1993**, *26*, 274.
2. Braña, M. F.; Ramos, A. *Curr. Med. Chem.—Anti-Cancer Agents* **2001**, *1*, 237.
3. Toshima, K.; Kimura, T.; Takano, R.; Ozawa, T.; Ariga, A.; Shima, Y.; Umezawa, K.; Matsumura, S. *Tetrahedron* **2003**, *59*, 7057.
4. Pindur, U.; Haber, M.; Sattler, K. *J. Chem. Edu.* **1993**, *70*, 263.
5. Becker, H. C.; Norden, B. *J. Am. Chem. Soc.* **2000**, *122*, 8344.
6. a Onfelt, B.; Lincoln, P.; Norden, B. *J. Am. Chem. Soc.* **2001**, *123*, 3630; b Yakovleva, L.; Handy, C. J.; Sayer, J. M.; Pirrung, M.; Jerina, D. M.; Shuman, S. *J. Biol. Chem.* **2004**, *279*, 23335; c Shi, S.; Liu, J.; Li, J.; Zheng, K. C.; Tan, C. P.; Chen, L. M.; Ji, L. N. *Dalton Trans.* **2005**, 2038; d Uerpmann, C.; Malina, J.; Pascu, M.; Clarkson, G. J.; Moreno, V.; Rodger, A.; Grandas, A.; Hannon, M. *Chem. Eur. J.* **2005**, *11*, 1750; e Jaramillo, D.; Buck, D. P.; Collins, J. G.; Fenton, R. R.; Stootman, F. H.; Wheate, N. J.; Aldrich-Wright, J. R. *Eur. J. Inorg. Chem.* **2006**, 839; (f) Montana, A. M.; Bernal, F. J.; Lorenzo, J.; Farnos, C.; Batalla, C.; Prieto, M. J.; Moreno, V.; Aviles, F. X.; Mesase, J. M.; Alegree, M.-T. *Bioorg. Med. Chem.* **2008**, *16*, 1721; g Han, F. S.; Osajima, H.; Cheung, M.; Tokuyama, H.; Fukuyama, T. *Chem. Eur. J.* **2007**, *13*, 3026.
7. Qu, X.; Trent, J. O.; Fokt, I.; Priebe, W. J.; Chaires, B. *Proc. Natl. Acad. Sci. U.S.A.* **2000**, *97*, 12032.
8. Eker, F.; Griebenow, K.; Schweitzer-Stenner, R. *J. Am. Chem. Soc.* **2003**, *125*, 8178.
9. Singh, M. P.; Plouvier, B. G.; Hill, C.; Gueck, J.; Richard, T.; Pon, J.; William, L. *J. Am. Chem. Soc.* **1994**, *116*, 7006.
10. a Zinchenko, A. A.; Sergeyev, V. G.; Kabanov, V. A., et al *Angew. Chem. Int. Ed.* **2004**, *43*, 2378; b Kochevar, E. D.; Dunn, D. In *Bioorganic Photochemistry*; Morrison, H., Ed.; John Wiley & Sons: New York, 1990; pp 83–273.
11. a Li, Z.; Yang, Q.; Qian, X. *Bioorg. Med. Chem. Lett.* **2005**, *15*, 3143; b Li, Z.; Yang, Q.; Qian, X. *Bioorg. Med. Chem.* **2005**, *15*, 4864; c Yin, H.; Xu, Y.; Qian, X. *Bioorg. Med. Chem.* **2007**, *15*, 1356; d Yang, P.; Yang, Q.; Qian, X. *Tetrahedron* **2005**, *61*, 11895; e Yang, P.; Yang, Q.; Qian, X. *Bioorg. Med. Chem.* **2005**, *13*, 5909; f Li, Z.; Yang, Q.; Qian, X. *Tetrahedron* **2005**, *61*, 8711; g Li, Z.; Yang, Q.; Qian, X. *Bioorg. Med. Chem. Lett.* **2005**, *15*, 1769; h Yin, H.; Xu, Y.; Qian, X. *Bioorg. Med. Chem. Lett.* **2007**, *17*, 2166; i Qian, X.; Li, Z.; Yang, Q. *Bioorg. Med. Chem.* **2007**, *15*, 6846.
12. Zhu, H.; Huang, M.; Yang, F.; Chen, Y.; Miao, Z.; Qian, X.; Xu, Y.; Qin, Y.; Luo, H.; Shen, X.; Geng, M.; Cai, Y.; Ding, J. *Molec. Cancer Therapeut.* **2007**, *6*, 484.
13. Li, Y.; Xu, Y.; Qian, X.; Qu, B. *Bioorg. Med. Chem. Lett.* **2003**, *13*, 3513.
14. Qian, X.; Li, Y.; Xu, Y.; Qu, B. *Bioorg. Med. Chem. Lett.* **2004**, *14*, 2665.
15. Xu, Y.; Qu, B.; Qian, X.; Li, Y. *Bioorg. Med. Chem. Lett.* **2005**, *15*, 1139.
16. **Ax**: 204.1–204.5 °C. ^{1}H NMR ($CDCl_3$) δ (ppm): 1.40 (s, br, 3H), 1.86–2.10 (m, 4H), 2.53 (s, br, 1H), 2.79 (s, br, 1H), 3.22–3.51 (m, br, 3H), 4.40 (s, br, 1H), 4.63 (s, br, 1H), 7.59–7.62 (m, 3H), 7.91–7.95 (dd, J_1 = 7.6 Hz, J_2 = 7.6 Hz, 1H), 8.35–8.38 (m, 2H), 8.66–8.68 (m, 2H), 9.01 (s, 1H), ESI-HRMS: calcd for $C_{26}H_{23}N_3O_3$ ($M+H^+$): 426.1818, found: 426.1814. IR (KBr): 3062, 2962, 2853, 1702, 1662, 1345 cm^{-1}.
A_R: 194.4–194.9 °C.^{1}H NMR ($CDCl_3$) δ (ppm): 1.39 (s, br, 3H), 1.85–2.09 (m, 4H), 2.56 (s, br, 1H), 2.79 (s, br, 1H), 3.25–3.52 (m, 3H), 4.36–4.39 (m, 1H), 4.62 (s, br, 1H), 7.60–7.62 (m, 3H), 7.91–7.95 (dd, J_1 = 7.6 Hz, J_2 = 7.6 Hz, 1H), 8.35–8.37 (m, 2H), 8.65–8.67 (m, 2H), 9.00 (s, 1H), ESI-HRMS: calcd for $C_{26}H_{23}N_3O_3$ ($M+H^+$): 426.1818, found: 426.1830; IR (KBr): 3062, 2964, 2798, 1701, 1662, 1361 cm^{-1}. [α] = +15.91 (C = 0.002, $CHCl_3$).
A_S: 182.3–183.8 °C. ^{1}H NMR (CDCl3) δ (ppm): 1.26–1.30 (t, J = 6.4 Hz, 3H), 1.81–2.02 (m, 4H), 2.44 (s, br, 1H), 2.66 (s, br, 1H), 3.12 (s, br, 1H), 3.25 (s, br, 1H), 3.41 (s, br, 1H), 4.26–4.30 (m, 1H), 4.48–4.51 (m, 1H), 7.58–7.61 (m, 3H), 7.89–7.93 (dd, J_1 = 8.0 Hz, J_2 = 7.6 Hz, 1H), 8.33–8.36 (m, 2H), 8.63–8.66 (m, 2H), 8.98 (s, 1H), ESI-HRMS: Calcd for $C_{26}H_{23}N_3O_3$ ($M+H^+$): 426.1818, found: 426.1801. IR (KBr): 3061, 2964, 2799, 1701, 1662, 1362 cm^{-1}. [α] = −18.74 (C = 0.002, $CHCl_3$).
Bx: 219.2–219.5 °C. 1H NMR (d_6-DMSO) δ (ppm): 1.06–1.10 (t, J = 7.6 Hz, 3H), 1.63–1.76 (m, 4H), 2.19 (s, br, 1H), 2.37–2.41 (m, 1H), 2.87–2.95 (m, 2H), 3.06 (s, br, 1H), 3.97–4.00 (m, 1H), 4.08–4.13 (m, 1H), 7.62–7.66 (m, 2H), 7.93–7.96 (dd, J_1 = 7.6 Hz, J_2 = 8.0 Hz, 1H), 8.21 (s, br, 1H), 8.50–8.52 (d, J = 7.6 Hz, 1H), 8.56–8.62 (m, 2H), 9.24 (s, 1H), ESI-HRMS: calcd for $C_{25}H_{22}N_2O_2S$ ($M+H^+$): 415.1480, found: 415.1469 IR (KBr): 2963, 2796, 1698, 1657, 1330 cm^{-1}.
B_R: 215.1–215.2 °C.^{1}H NMR (d_6-DMSO) δ (ppm): 1.23 (s, br, 3H), 1.83 (s, br, 4H), 3.21 (s, br, 4H), 3.62 (s, br, 1H), 4.41 (s, br, 2H), 7.67–7.70 (m, 2H), 8.02–8.05 (dd, J_1 = 8.4 Hz, J_2 = 6.8 Hz, 1H), 8.28–8.30 (m, 1H), 8.59–8.61(d, J = 7.2 Hz, 1H), 8.72–8.73 (m, 2H), 9.40 (s, 1H), ESI-HRMS: calcd for $C_{25}H_{22}N_2O_2S$ ($M+H^+$): 415.1480, found: 415.1481, IR (KBr): 3054, 2963, 2796, 2621, 1698, 1659, 1335 cm^{-1}. [α] = +6.63 (C = 0.002, $CHCl_3$).
B_S: 222.6–222.7 °C.^{1}H NMR (d_6-DMSO) δ (ppm): 1.23 (s, br, 3H), 1.76 (s, br, 4H), 2.99–3.18 (m, 3H), 3.32–3.42 (m, 2H), 4.13–4.16 (m, 1H), 4.43–4.50 (m, 1H), 7.66–7.69 (m, 2H), 8.01–8.03 (dd, J_1 = 8.0 Hz, J_2 = 8.0 Hz, 1H), 8.26–8.28 (m, 1H), 8.58–8.60 (d, J = 6.0 Hz, 1H), 8.70 (s, br, 2H), 9.37 (s, 1H), ESI-HRMS: calcd for $C_{25}H_{22}N_2O_2S$ ($M+H^+$): 415.1480, found: 415.1497 IR (KBr): 3052, 2963, 1697, 1659, 1335 cm^{-1}. [α] = −3.54 (C = 0.001, $CHCl_3$).
Cx: 210.0–211.0 °C. ^{1}H NMR (d_6-DMSO) δ (ppm): 1.14–1.17 (t, J = 7.6 Hz, 3H), 1.72–1.89 (m, 4H), 2.60–2.73 (m, 2H), 3.10–3.40 (m, 3H), 4.14–4.22 (m, 2H), 7.46–7.57 (m, 3H), 7.70–7.72 (d, J = 8.8 Hz, 1H), 8.29–8.31 (d, J = 8.0 Hz, 1H), 8.41–8.50 (m, 3H), ESI-HRMS: calcd for $C_{25}H_{22}N_2O_2S$ ($M+H^+$): 415.1480, found: 415.1487; IR (KBr): 2964, 1690, 1647, 1368 cm^{-1}.
C_R: 217.2–217.9 °C. ^{1}H NMR (d_6-DMSO) δ (ppm): 1. 33 (s, br, 3H), 1.73–1.94 (m, 3H), 2.13 (s, br, 1H), 3.17 (s, br, 2H), 3.60 (s, br, 3H), 4.37 (s, br, 1H), 4.49 (s, br, 1H), 7.49–7.59 (m, 3H), 7.73–7.75 (d, J = 7.6 Hz, 1H), 8.33–8.35 (d, J = 7.6 Hz, 1H), 8.44–8.53 (m, 3H), ESI-HRMS: calcd for $C_{25}H_{22}N_2O_2S$ ($M+H^+$): 415.1480, found: 415.1476 IR (KBr): 2964, 1690, 1649, 1369 cm^{-1}. [α] = +5.91 (C = 0.001, $CHCl_3$).
C_S: 198.4–198.6 °C. ^{1}H NMR (d_6-DMSO) δ (ppm): 1.23 (s, br, 3H), 1.75–1.97 (m, 4H), 2.86 (s, br, 2H), 3.34–3.52 (m, 3H), 4.20 (s, br, 1H), 4.34 (s, br, 1H), 7.48–7.58 (m, 3H), 7.74–7.76 (d, J = 8.0 Hz, 1H), 8.31–8.33 (d, J = 8.4 Hz, 1H), 8.45–8.50 (m, 3H); ESI-HRMS: calcd for $C_{25}H_{22}N_2O_2S$ ($M+H^+$): 415.1480, found: 415.1481; IR (KBr): 2964, 1688, 1648, 1366 cm^{-1}. [α] = −4.65 (C = 0.001, $CHCl_3$).
Dx: M.p.: 204.9–205.2 °C. ^{1}H NMR (d_6-DMSO) δ (ppm): 1.32 (s, 3 H), 1.84–2.08 (m, 4 H), 2.22 (m, 1 H), 2.39 (m, 1 H), 3.18 (br, 1 H), 3.63–3.77 (m, 2H), 4.41–4.57 (br, 2 H), 7.67 (m, 3 H), 8.04–8.08 (t, J_1 = 8.0 Hz, J_2 = 7.6 Hz, 1 H), 8.22–8.23 (m, 2 H), 8.60–8.61 (d, J = 7.2 Hz, 1 H), 8.71–8.73 (d, J = 8.4 Hz, 1 H), 9.00 (s, 1 H). ESI-HRMS: calcd for $C_{26}H_{23}N_3O_2S$ ($M+H^+$): 442.1589, found: 442.15997. IR (KBr): 3063, 2938, 2873, 1699, 1655, 1348 cm^{-1}.
D_R: Mp.: 198.9–199.3 °C. ^{1}H NMR (d_6-DMSO) δ (ppm): 1.29 (s, 3 H), 1.87 (br, s, 4 H), 2.21 (br, 1 H), 2.392 (br, 1 H), 3.18 (br, 1 H), 3.62 (br, s, 2 H), 4.44 (br, 1 H), 4.57 (br, s, 1 H), 7.63–7.66 (m, 3 H), 8.02–8.03 (t, J_1 = 8.0 Hz, J_2 = 7.6 Hz, 1 H), 8.20–8.22 (m, 2 H), 8.60–8.58 (d, J = 8.8 Hz, 1 H), 8.69–8.71 (d, J = 8.0 Hz, 1 H), 8.98 (s, 1 H). [α] = +13.54 (C = 0.001, $CHCl_3$). ESI-HRMS: calcd for $C_{26}H_{23}N_3O_2S$ ($M+H^+$): 442.1589, found: 442.1589. IR (KBr): 3062, 2964, 1699, 1659, 1332 cm^{-1}.
D_S: Mp.: 178.9–179.4 °C. ^{1}H NMR (d_6-DMSO) δ (ppm): 1.33–1.37 (t, J_1 = 7.6 Hz, J_2 = 6.8 Hz, 3 H), 1.84–2.08 (m, 4 H), 2.21 (m, 1 H), 2.38 (m, 1 H), 3.18 (br, 1 H), 3.62–3.77 (m, 2 H), 4.41–4.44 (m, 1 H), 4.52–4.58 (m, 1 H), 7.67 (m, 3 H), 8.04–8.08 (t, J_1 = 8.4 Hz, J_2 = 7.6 Hz, 1 H), 8.22–8.23 (m, 2 H), 8.60–8.62 (d, J = 7.6 Hz, 1 H), 8.72–8.74 (d, J = 8.0 Hz, 1 H), 9.00 (s, 1 H); [α] = −6.54 (C = 0.001, $CHCl_3$). ESI-HRMS: calcd for $C_{26}H_{23}N_3O_2S$ ($M+H^+$): 442.1589, Found: 442.1576. IR (KBr): 2923, 2852, 1701, 1661, 1334 cm^{-1}.
17. Gupta, M.; Ali, R. *J. Biochem.* **1984**, *95*, 1253.